Science Advances
AAAS

Supplementary Materials for

SNARE assembly enlightened by cryo-EM structures of a synaptobrevin–Munc18-1–syntaxin-1 complex

Karolina P. Stepien *et al.*

Corresponding author: Josep Rizo, jose.rizo-rey@utsouthwestern.edu;
Xiao-Chen Bai, xiaochen.bai@utsouthwestern.edu

Sci. Adv. **8**, eabo5272 (2022)
DOI: 10.1126/sciadv.abo5272

This PDF file includes:

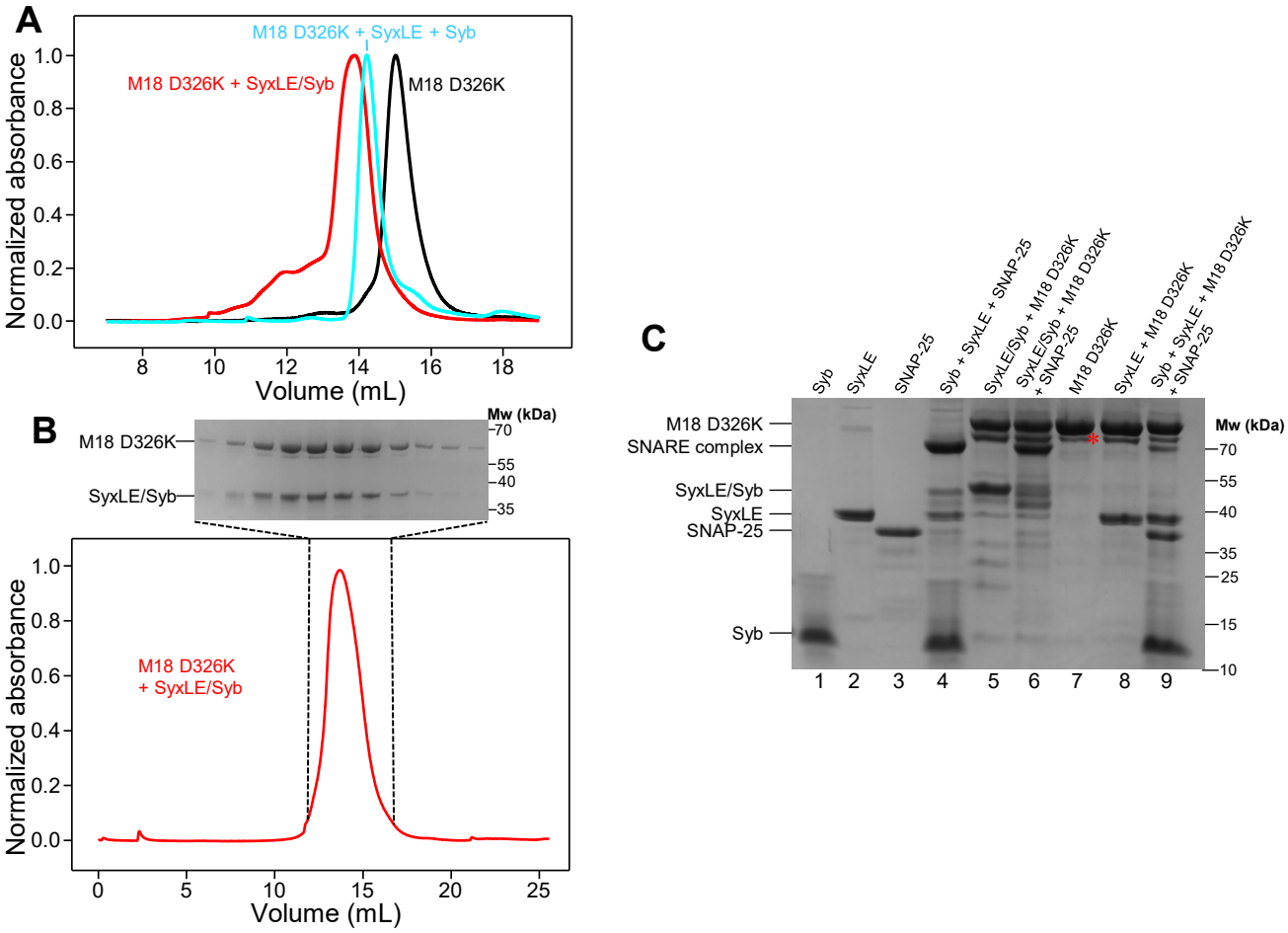

Fig. S1. Preparation of the template complex. (**A**) Gel filtration on Superdex S200 of Munc18-1 D326K alone (black curve) or after overnight incubation with SyxLE/Syb (red curve) or after overnight incubation with non-cross-linked SyxLE plus Syb (blue curve). The absorbance at 280 nm was normalized to the maximum absorbance observed in each chromatogram. (**B**) Gel filtration of an equimolar mixture of Munc18-1 D326K and SyxLE/Syb used to purify the template complex. SDS-PAGE analysis of the eluted fractions containing the complex is shown above the chromatogram. (**C**) SDS-PAGE analysis of SNARE complex assembly. The lanes were loaded with different mixtures Syb, SyxLE, SNAP-25, Munc18-1 D326K (M18 D326K) and SyxLE/Syb in different combinations as indicated at the top. All samples were incubated for three minutes at room temperature before loading onto the gel. Formation of the SDS-resistant SNARE complex was much more efficient for the mixture containing SyxLE/Syb, SNAP-25 and M18 D326K (lane 6) than that containing Syb, SyxLE, SNAP-25 and M18 D326K (lane 9). The positions of the proteins and complexes are indicated on the left, and those of molecular weight markers on the right. A common degradation band of Munc18-1 is indicated with a *, but note that such degradation is common in Munc18-1 and does not prevent syntaxin-1 binding (*8*).

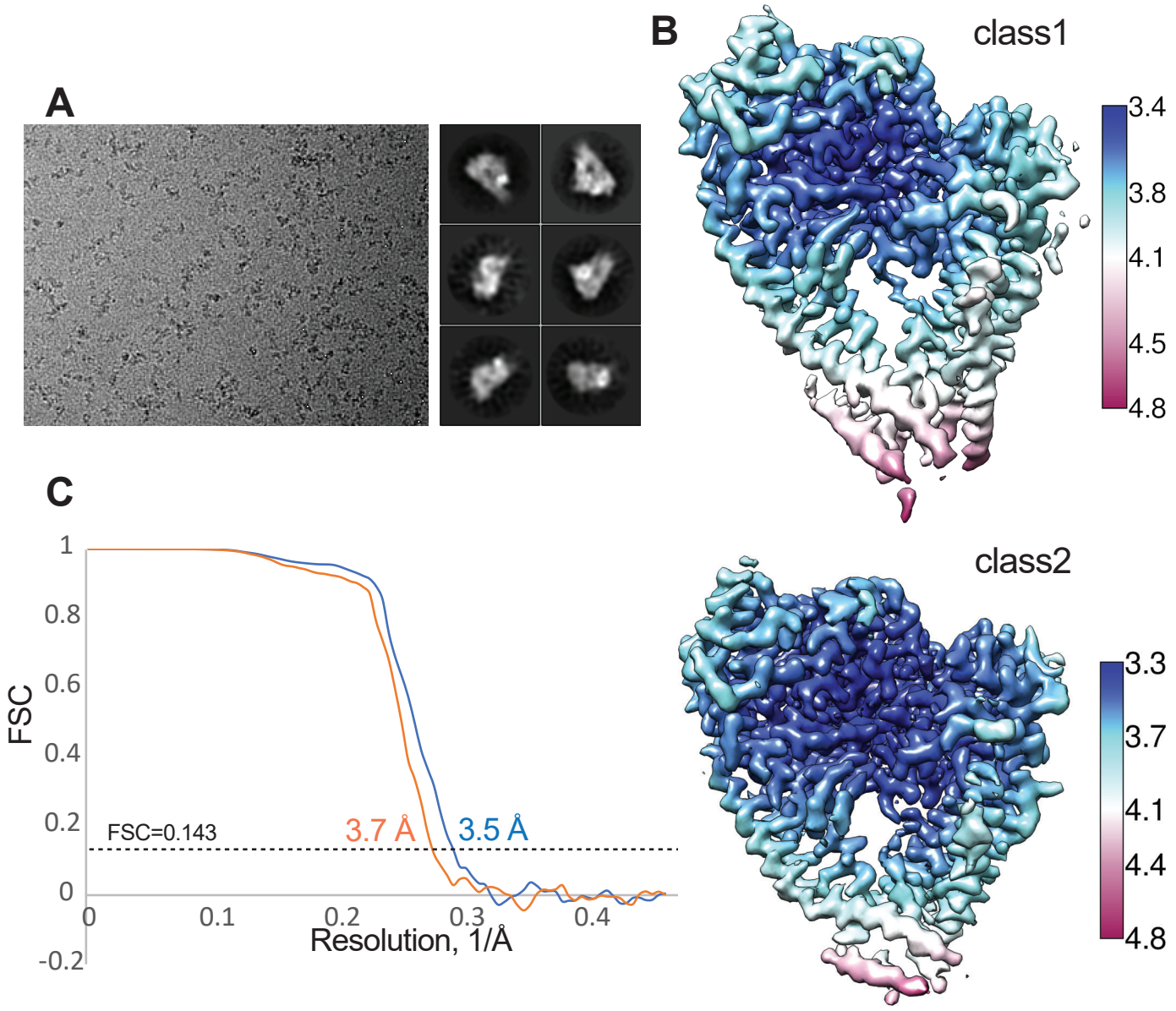

Figure S2. Cryo-EM analysis of the template complex. (**A**) Representative electron micrograph from a total 7,401 images acquired and 2D class averages of the template complex. (**B**) Cryo-EM maps of the two conformers of the template complex (class1 and class2) colored by local resolution. The color scales are in Å (**C**). Gold-standard Fourier shell correlation (FSC) curve for the cryo-EM maps of the template complex. Red: class1; blue: class2.

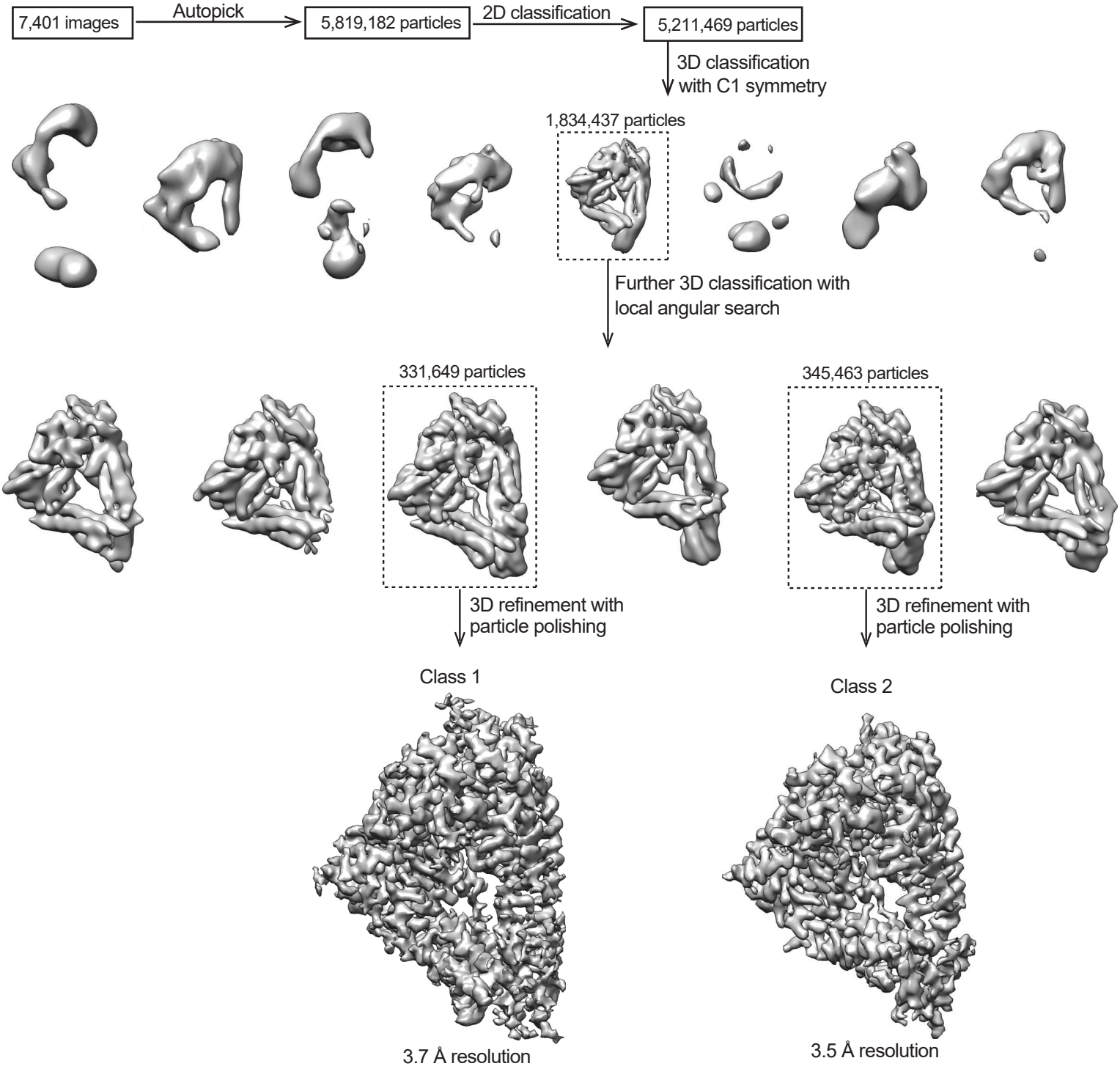

Figure S3. Flow-chart of cryo-EM data processing leading to the two conformers of the template complex (class1 and class2).

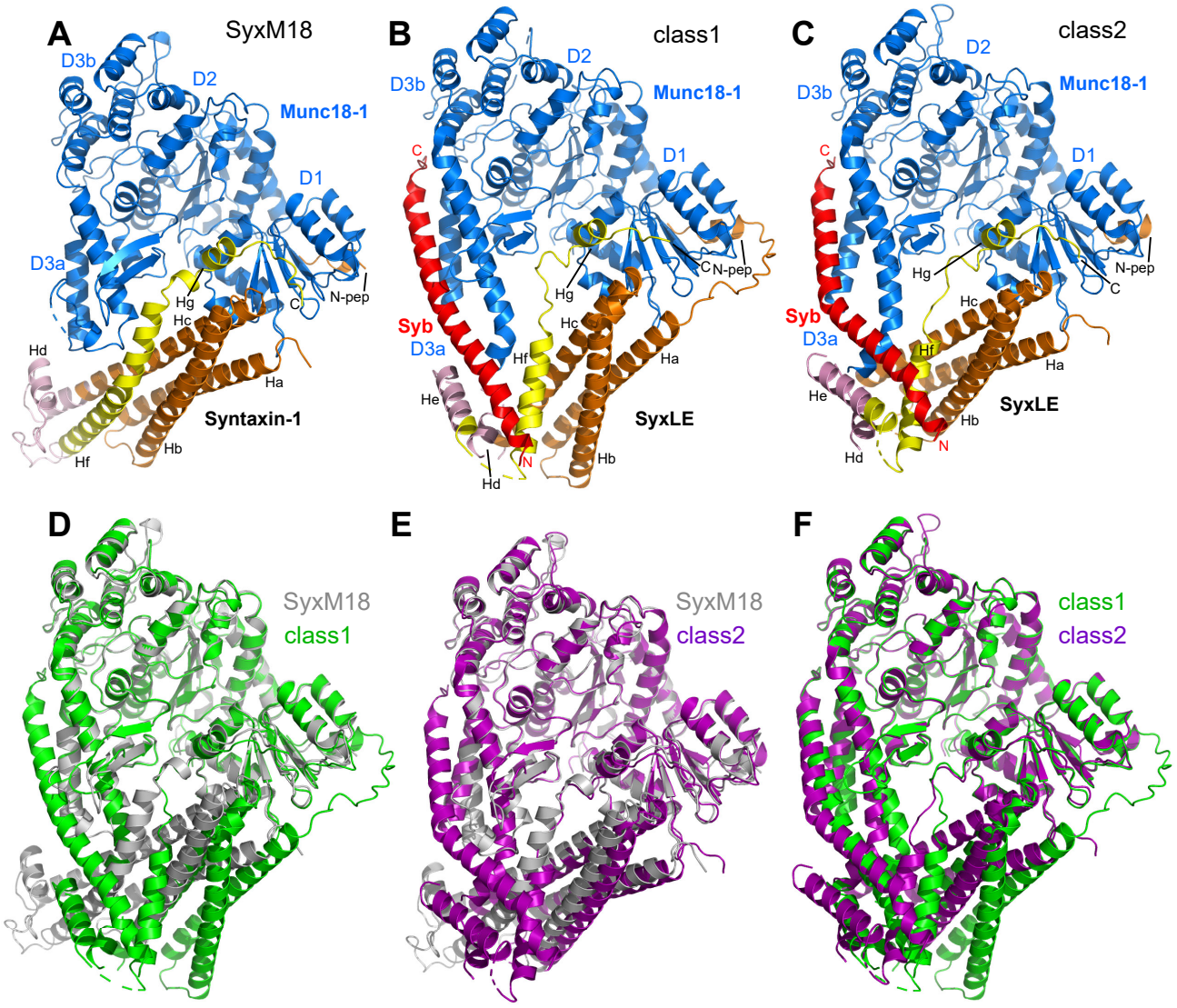

Figure S4. Structural comparison of class1, class2 and the syntaxin-1-Munc18-1 complex (SyxM18). (**A-C**) Ribbon diagrams of the structures of the syntaxin-1-Munc18-1 complex (SyxM18) (PDB code 3C98) (*8, 34*) (**A**), class1 (**B**) and class2 (**C**). The color code is the same as in Fig. 1D-F. The domains of Munc18-1 (D1, D2, D3a and D3b) are labeled. The syntaxin-1 helices are indicated (named Ha-Hg). (**D-F**) Superpositions of ribbon diagrams of SyxM18 (grey), class1 (green) and class2 (purple) using the Munc18-1 Cα atoms for the superpositions. The root mean square (r.m.s.) deviations were the following: Munc18-1 versus class1 (**D**) 0.59 Å for 470 Cα carbons; Munc18-1 versus class2 (**E**) 0.54 Å for 455 Cα carbons; and class1 versus class2 (**F**) 0.38 Å for 474 Cα carbons.

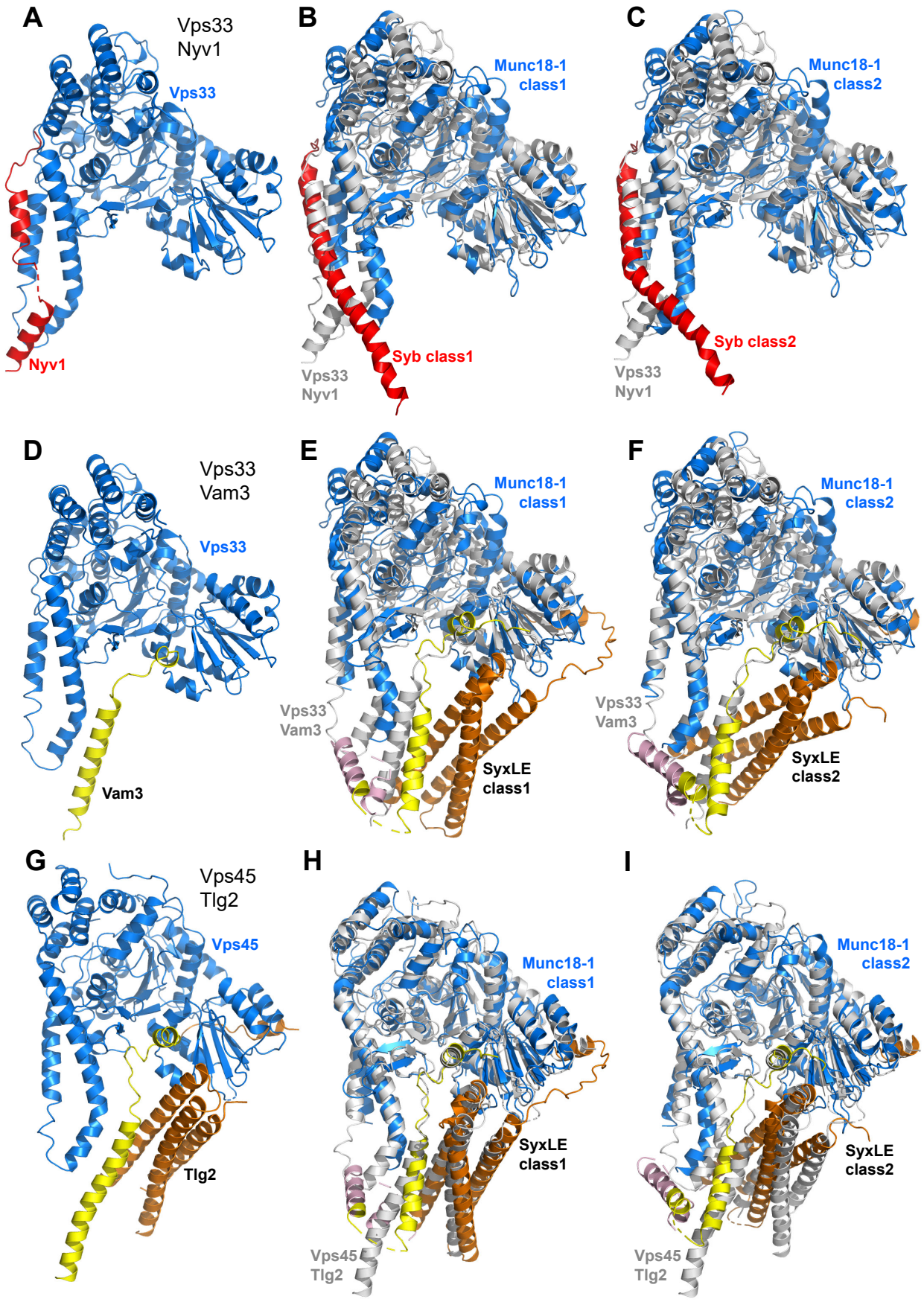
A
Vps33
Nyv1
Vps33
Nyv1
B
Munc18-1
class1
Syb class1
Vps33
Nyv1
C
Munc18-1
class2
Syb class2
Vps33
Nyv1
D
Vps33
Vam3
Vps33
Vam3
E
Munc18-1
class1
Vps33
Vam3
SyxLE
class1
F
Munc18-1
class2
Vps33
Vam3
SyxLE
class2
G
Vps45
Tlg2
Vps45
Tlg2
H
Munc18-1
class1
SyxLE
class1
Vps45
Tlg2
I
Munc18-1
class2
SyxLE
class2
Vps45
Tlg2

Figure S5. Structural comparisons of class1 and class 2 with the Vps33/Nyv1, Vpss33/Vam3 and Vps45/Tlg2 complexes. (**A**,**D**,**G)** Ribbon diagrams of the structures of the Vps33-Nyv1 complex (PDB code 5BV0) (*30*) (**A**), the Vps33-Vam3 complex (PDB code 5BUZ) (*30*) (**D**) and the Vps45-Tlg complex (PDB code 6XMD) (*35*) (**G**). Note that the Vps33-Nyv1 and Vps33-Vam3 complexes also included Vps16, which is not shown for simplicity. Vps33 and Vps45 are shown in blue, Nyv1 in red, the Vam3 SNARE motif in yellow, and Tlg2 in orange (H_{abc} domain) and yellow (SNARE motif). (**B**,**C**,**E**,**F**,**H**,**I**) Superpositions of class1 and class2 with Vps33-Nyv1 (**B**,**C**), Vps33-Vam3 (**E**,**F**) and Vps45-Tlg2 (**H**,**I**). Vps33-Nyv1, Vps33-Vam3 and Vps45-Tlg2 are shown in gray. The color code for class1 and class 2 is the same as in Fig. 1. The superpositions per performed using corresponding Cα carbons of the SM proteins, yielding the following r.m.s. deviations: Vps33-Nyv1 versus class1: 4.91 Å for 394 Cα carbons; Vps33-Nyv1 versus class2: 5.18 Å for 411 Cα carbons; Vps33-Vam3 versus class1 4.47 Å for 379 Cα carbons; Vps33-Vam3 versus class2 4.99 Å for 406 Cα carbons; Vps45-Tlg2 versus class1 1.67 Å for 323 Cα carbons; and Vps45-Tlg2 versus class2 1.80 Å for 323 Cα carbons.

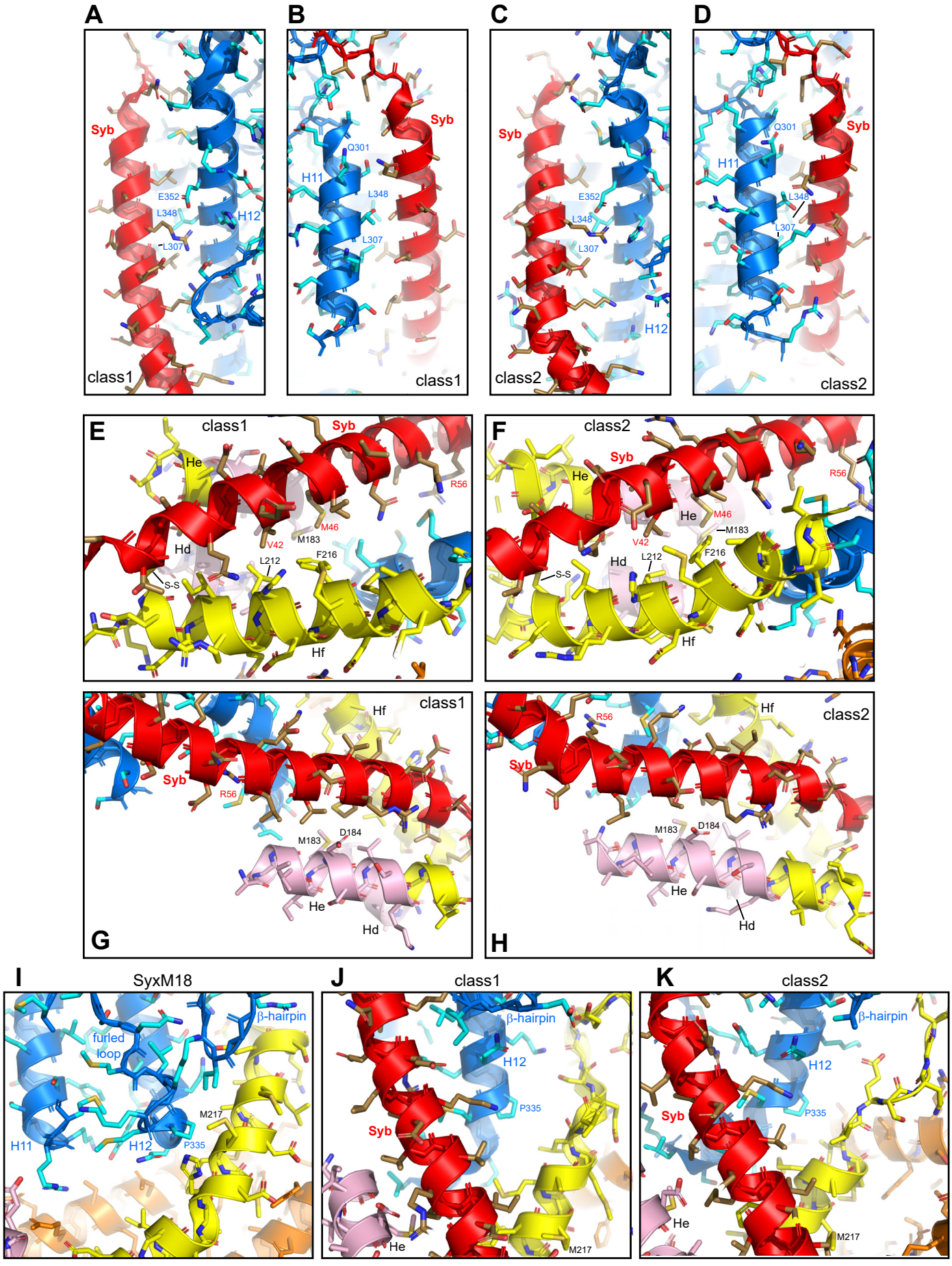
A
Syb
E352
L348
H12
L307
class1
B
Syb
Q301
H11
L348
L307
class1
C
Syb
E352
L348
L307
H12
class2
D
Q301
Syb
H11
L348
L307
class2
E
class1
Syb
He
R56
M46
M183
Hd
V42
F216
L212
S-S
Hf
F
class2
Syb
He
R56
He
M46
M183
V42
F216
Hd
L212
S-S
Hf
G
class1
Hf
Syb
R56
M183
D184
He
Hd
H
class2
R56
Hf
Syb
M183
D184
He
Hd
I
SyxM18
β-hairpin
furled loop
M217
H11
H12
P335
J
class1
β-hairpin
H12
P335
Syb
He
M217
K
class2
β-hairpin
H12
P335
Syb
He
M217

Figure S6. Interactions between different structural elements of Munc18-1, synaptobrevin and syntaxin-1 in class1 and class2. (**A**-**K**) The diagrams show close-up views of the regions where: synaptobrevin binds to Munc18-1 in class1 (**A**,**B**) and class2 (**C**,**D**); the syntaxin-1 linker forms a small four-helix bundle with the syntaxin-1 and synaptobrevin SNARE motifs in class1 (**E**,**G**) or class2 (**F**,**H**); P335 and a β-hairpin of Munc18-1 interact with or are close to the syntaxin-1 motif in the syntaxin-1-Munc18-1 complex (SyxM18) (**I**), class1 (**J**) or class2 (**K**) The structures are represented with ribbon diagrams [Munc18-1 in blue; synaptobrevin (Syb) in red; syntaxin-1 in orange (N-peptide and H_{abc} domain), pink (linker) and yellow (SNARE motif)] and stick models with the following color code for side chain atoms: oxygen atoms red, nitrogen atoms blue, sulfur atoms light orange and carbon atoms in cyan for Munc18-1, brown for synaptobrevin and orange (H_{abc} domain), pink (linker) or yellow (SNARE motif) for syntaxin-1. The positions of selected residues discussed in the text, selected helices of syntaxin-1, the disulfide bond linking syntaxin-1 and synaptobrevin, the furled loop and the β-hairpin are indicated in the relevant panels. The M217 side chain is labeled in panels **I**-**K** to show that the SNARE motif of syntaxin-1 is shifted downwards in class1 and class2 with respect to its position in the syntaxin-1-Munc18-1 complex.

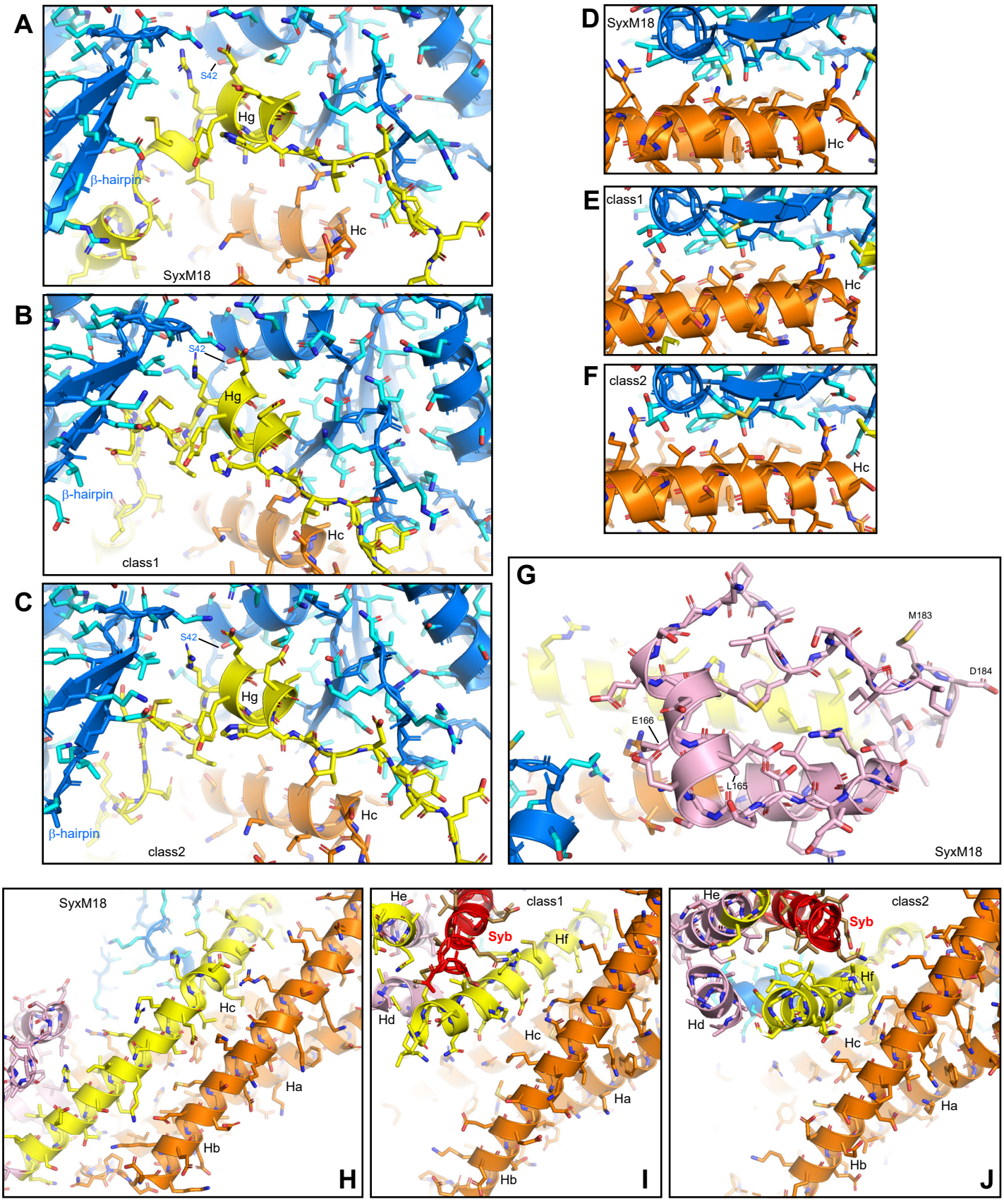
A
S42
Hg
β-hairpin
Hc
SyxM18
B
S42
Hg
β-hairpin
Hc
class1
C
S42
Hg
Hc
β-hairpin
class2
D
SyxM18
Hc
E
class1
Hc
F
class2
Hc
G
M183
D184
E166
L165
SyxM18
H
SyxM18
Hc
Ha
Hb
I
He
class1
Syb
Hf
Hd
Hc
Ha
Hb
J
He
class2
Syb
Hf
Hd
Hc
Ha
Hb

Figure S7. Comparison of interactions among Munc18-1, the syntaxin-1 SNARE motif and the H_{abc} domain in the syntaxin-1-Munc18-1 (SyxM18) complex, class1 and class2. The diagrams show cloase-up views of the regions where: the C-terminal half of the syntaxin-1 SNARE motif binds to the Munc18-1 cavity in the syntaxin-1-Munc18-1 complex (SyxM18) (**A**), class1 (**B**) or class2 (**C**); the syntaxin-1 H_{abc} domain binds to Munc18-1 in SyxM18 (**D**), class1 (**E**) or class2 (**F**); the syntaxin-1 linker packs against the SNARE motif in SyxM18 (**G**); and the syntaxin-1 SNARE motif interacts with the H_{abc} domain in SyxM18 (**H**), class1 (**I**) or class2 (**J**). The structures are represented with ribbon diagrams and stick models with the same color coding as Fig. S6. The positions of selected helices and residues discussed in the text are indicated in the relevant panels. Panel (**G**) shows that residues L165 and E166, which are replaced in the LE mutation, are buried in SyxM18.

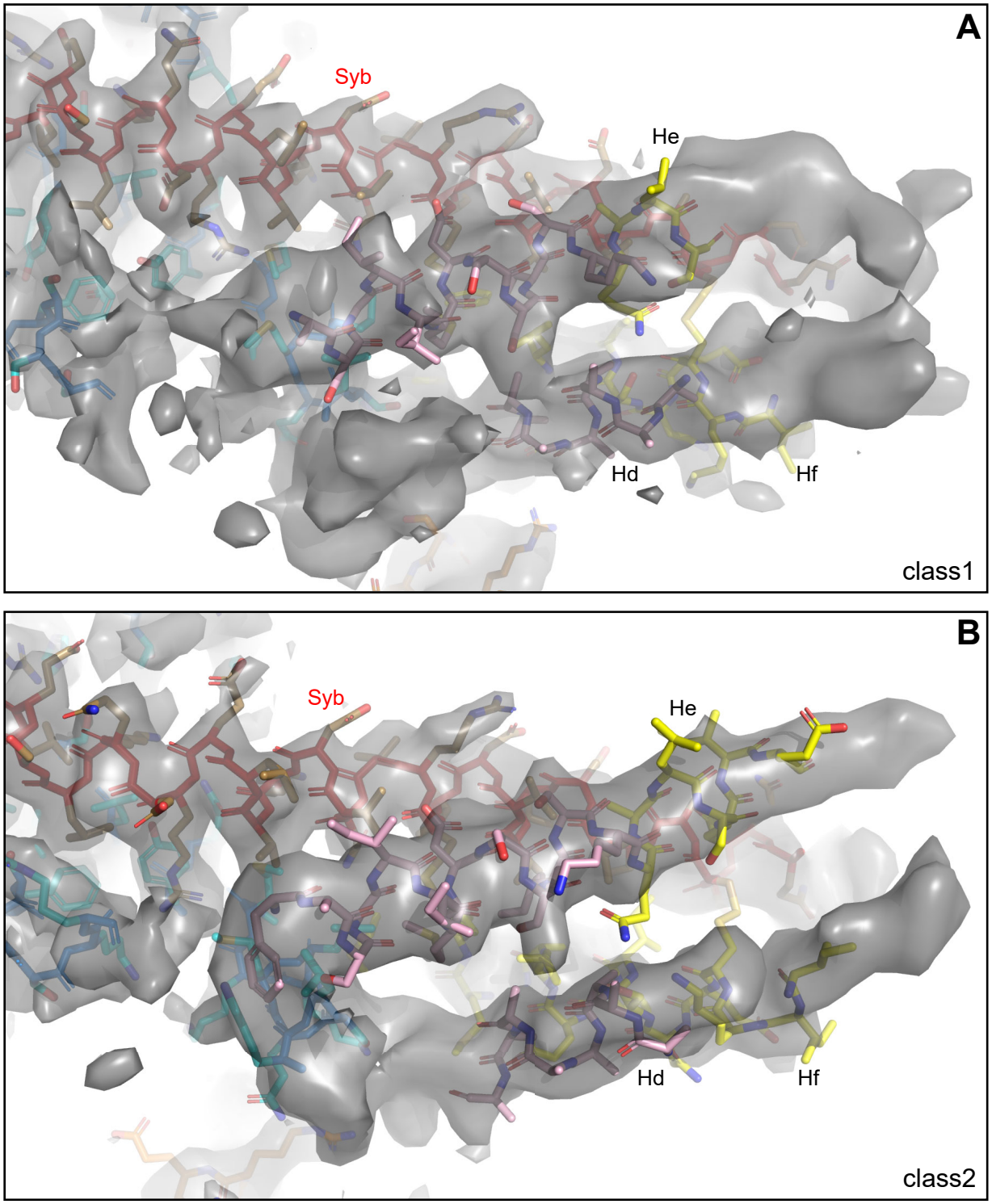

Fig. S8. Region around the short four-helix bundle of the Cryo-EM maps of class1 (**A**) and class2 (**B**). The modeled structures are represented by stick models with the same color coding as Fig. S6. The positions of the N-terminal half of the synaptobrevin SNARE motif (Syb) and helices Hd-Hf are indicated.

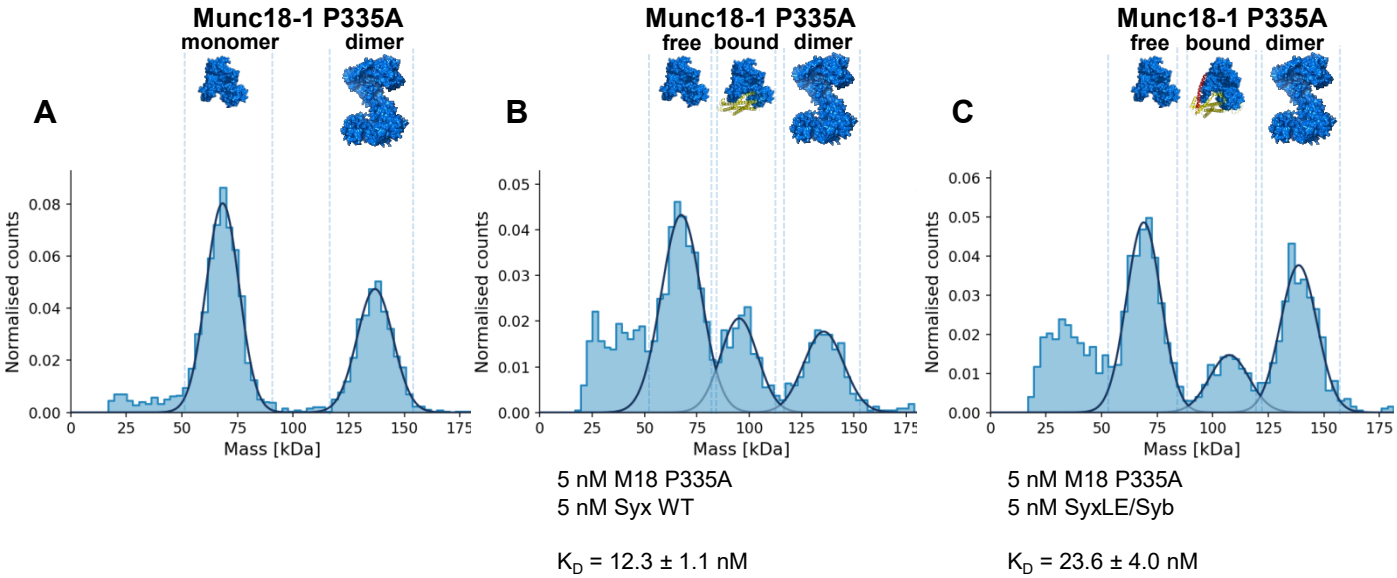

Figure S9. Analysis of Munc18-1 P335A mutant-SNARE interactions by mass photometry. (**A**-**C**) Normalized histograms of mass distributions observed for samples containing 5 nM Munc18-1 (M18) P335A mutant alone (**A**) or together with 5 nM WT syntaxin-1(2-253) (Syx) (**B**), or 5 nM SyxLE/Syb (**C**). Gaussian fits (solid lines) were used to calculate the populations of free and bound Munc18-1 P335A, and derive dissociation constants (K_Ds).

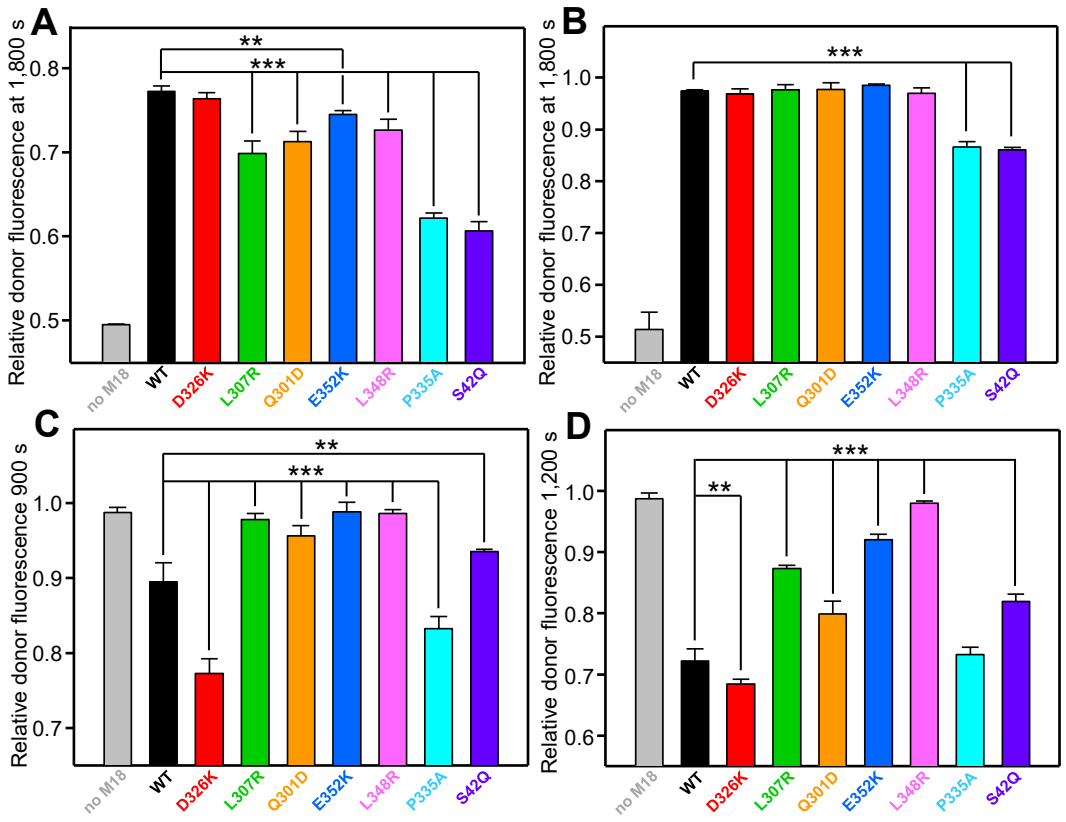

Figure S10. Quantification of the SNARE complex assembly assays at selected time points to highlight differences between the results obtained with different mutants. (**A**,**B**) Diagrams showing the relative donor fluorescence (normalized to the first time point) observed at 1,800 s in the SNARE complex assembly assays performed in solution with SyxMUN (**A**) or Syx (**B**) in the presence of WT or mutant Munc18-1 (corresponding to Fig. 4C and 4D, respectively). (**C**,**D**) Diagrams showing the relative donor fluorescence (normalized to the first time point) observed at 900 s, i.e. before Ca^{2+} addition (**C**), and at 1,200 s, i.e. after Ca^{2+} addition (**D**), in the trans-SNARE complex performed with WT or mutant Munc18-1 (corresponding to Fig. 4F). Bars represent averages of the normalized fluorescence intensities observed in three independent experiments. Error bars represent standard deviations. Statistical significance and p values were determined by one-way analysis of variance (ANOVA) with the Holm-Sidak test (*** $p < 0.001$, ** $p < 0.01$).

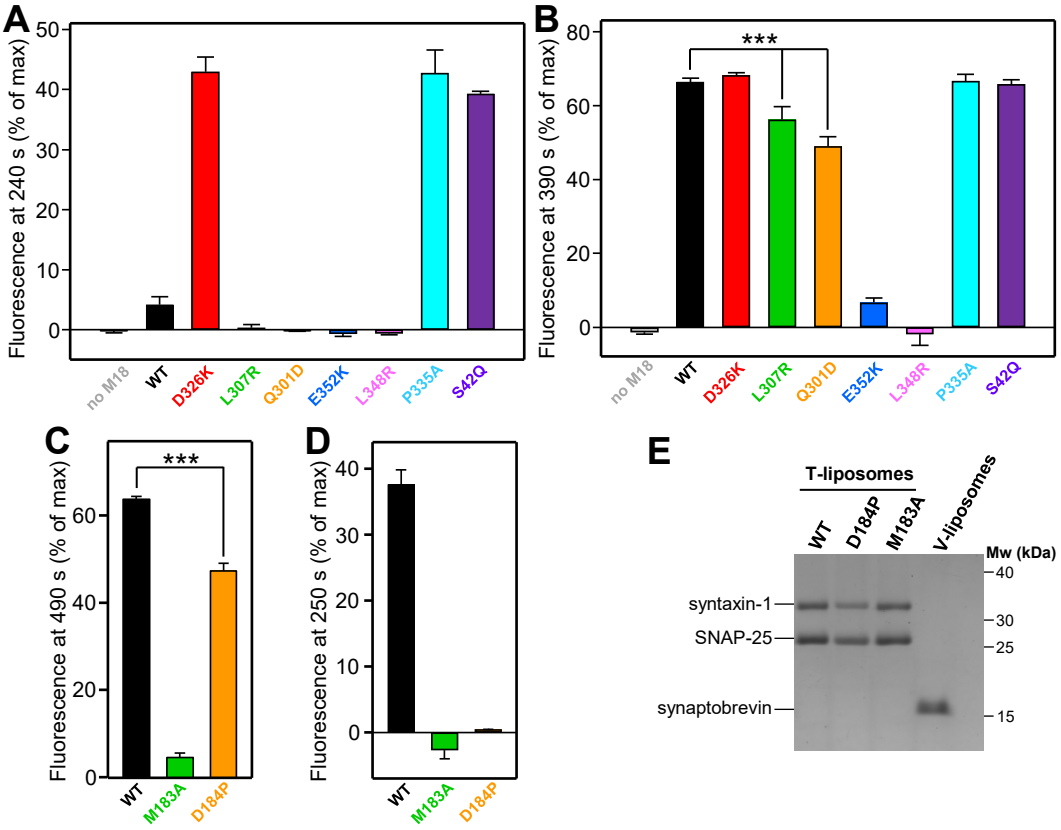

Figure S11. Quantification of the liposome fusion assays performed with different Munc18-1 and syntaxin-1 mutants. (**A**-**D**) Diagrams showing the relative fluorescence observed at 240 s, i.e. before Ca^{2+} addition (**A**), and at 390 s, i.e. after Ca^{2+} addition (**B**), in the content mixing assays performed with WT and mutant Munc18 (corresponding to Fig. 5B); at 490 s, i.e. after Ca^{2+} addition in the content mixing assays performed with WT Munc18-1 and WT or mutant syntaxin-1 (**C**) (corresponding to Fig. 5C); or at 250 s, i.e. before Ca^{2+} addition, in analogous assays performed with D326K mutant Munc18-1 and WT or mutant syntaxin-1 (**D**) (corresponding to Fig. 5D). Bars represent averages of the normalized fluorescence intensities observed in three independent experiments. Error bars represent standard deviations. Statistical significance and p values were determined by one-way analysis of variance (ANOVA) with the Holm-Sidak test (*** $p < 0.001$). (**E**) SDS-PAGE analysis of protein incorporation into V-liposomes and the T-liposomes containing WT or mutant syntaxin-1, which were used for the fusion assays of Fig. 5. The positions of the SNARE proteins are indicated on the left, and those of molecular weight markers on the right.

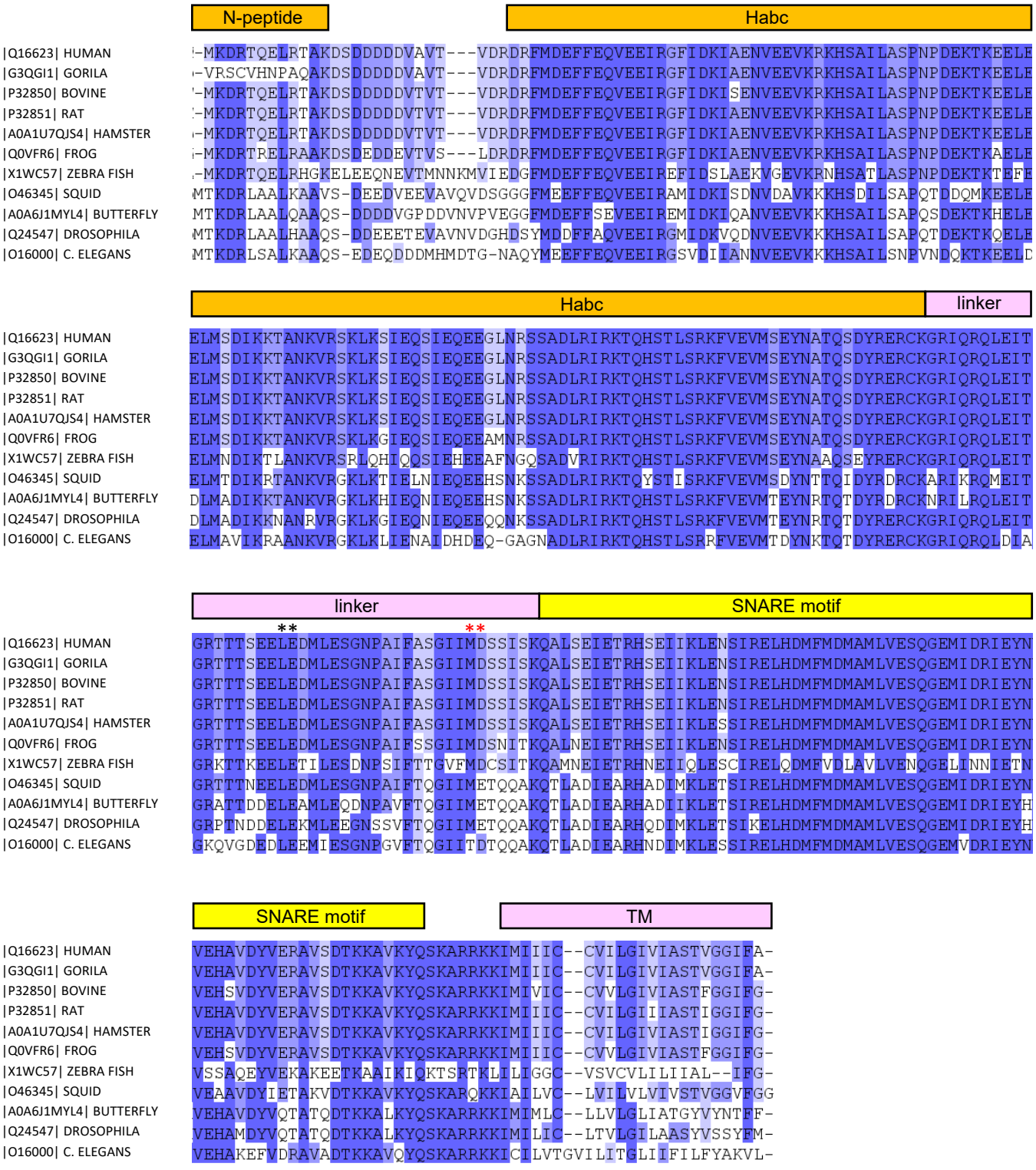

Figure S12. Sequence alignment of syntaxin-1A homologues from different species. The Uniprot (https://www.uniprot.org) code of each sequence and the common name of the species are indicated on the left. Conserved residues have a colored background. The color intensity reflects the degree of conservation. The domain diagram of syntaxin-1 with the same color code used in Fig. 1A is shown above the sequences. The positions of L165 and L166, which were mutated in the syntaxin-1 LE mutant, and of M183 and D184, the residues in the linker that were mutated, are indicated with *.

Supplementary Tables

Table S1. Cryo-EM data collection, refinement, and validation statistics.

	class2	class1
Data collection and processing		
Magnification	46,296	46,296
Voltage (kV)	300	300
Electron exposure (e–/Å2)	60	60
Defocus range (μm)	1.6 – 2.6	1.6 – 2.6
Pixel size (Å)	1.08	1.08
Symmetry imposed	C1	C1
Initial particle images (no.)	5,819,182	5,819,182
Final particle images (no.)	345,463	331,649
Map resolution (Å)	3.5	3.7
FSC threshold	0.143	0.143
Refinement		
Initial model used (PDB code)	3C98	3C98
Model composition		
Atoms	6472	6425
Protein residues	807	806
Ligands	0	0
R.m.s. deviations		
Bond lengths (Å)	0.003	0.003
Bond angles (°)	0.499	0.539
Validation		
MolProbity score	1.50	1.63
Clashscore	6.46	7.77
Poor rotamers (%)	0.14	0.28
Ramachandran plot		
Favored (%)	97.20	96.70
Allowed (%)	2.80	3.30
Disallowed (%)	0.00	0.00

Table S2. Buried accessible surface areas (Å^2) between different proteins and structural elements in class1, class2 and the Munc18-1-syntaxin-1 complex[a]

	Munc18-1 syntaxin-1	Munc18-1 synaptobrevin	Munc18-1 SyxLE/Syb	syntaxin-1 synaptobrevin	syntaxin-1 H_{abc} domain syntaxin-1 SNARE motif
class1	2810	1412	2097	660	509
class2	2743	1413	2067	680	438
SyxM18[b]	2703				1313

[a]Buried solvent accessible surface areas were calculated using Pymol (Schrödinger, LLC) adding hydrogen atoms and using high sampling density, with the parameter dot_solvent set to 1 and set dot_density set to 3.

[b]Syntaxin-1-Munc18-1 complex (PDB code 3C98)

Table S3. Summary of concentrations used for mass photometry experiments and measured K_Ds[a]

Protein 1	[Protein 1]	Protein 2	[Protein 2]	K_D (nM)
Munc18-1 WT	5 nM, 5 nM	syntaxin-1 WT	2.5 nM, 5 nM	3.3 ± 0.5
Munc18-1 P335A	5 nM, 5 nM	syntaxin-1 WT	2.5 nM, 5 nM	12.3 ± 1.1
Munc18-1 S42Q	5 nM, 10 nM	syntaxin-1 WT	5 nM, 5 nM	67.9 ± 4.3
Munc18-1 WT	5 nM, 5 nM	syntaxin-1 M183A	2.5 nM, 5 nM	0.6 ± 0.2
Munc18-1 WT	5 nM, 5 nM	syntaxin-1 D184P	2.5 nM, 5 nM	1.9 ± 0.2
Munc18-1 D326K	5 nM, 5 nM	SyxLE/Syb	2.5 nM, 5 nM	9.4 ± 0.2
Munc18-1 WT	5 nM, 5 nM	SyxLE/Syb	2.5 nM, 5 nM	17.9 ± 1.0
Munc18-1 D326K	30 nM, 35 nM	SyxLE M183A/Syb	15 nM, 35 nM	n.d.[b]
Munc18-1 D326K	30 nM, 35 nM	SyxLE D184P/Syb	15 nM, 35 nM	n.d.[b]
Munc18-1 P335A	5 nM, 5 nM	SyxLE/Syb	2.5 nM, 5 nM	23.6 ± 4.0
Munc18-1 S42Q	35 nM, 30 nM	SyxLE/Syb	35 nM, 15 nM	267 ± 28
Munc18-1 L307R	20 nM, 20 nM	SyxLE/Syb	10 nM, 20 nM	72.2 ± 1.7
Munc18-1 Q301D	20 nM, 20 nM	SyxLE/Syb	10 nM, 20 nM	90.6 ± 5.2
Munc18-1 E352K	10 nM, 20 nM	SyxLE/Syb	10 nM, 10 nM	97.8 ± 5.5
Munc18-1 L348R	20 nM, 30 nM	SyxLE/Syb	20 nM, 15 nM	140 ± 137

[a]Six experiments were performed for each pair of proteins, 3 at the first concentrations indicated in the [Protein 1] and [Protein 2] columns, and 3 at the second concentrations listed. The six K_D values obtained where used to calculated the listed average K_D ± standard deviation.

[d]Binding was too weak to derive accurate K_Ds (n.d. = not determined)